Proc. NIPR Symp. Antarct. Meteorites, **9**, 97–110, 1996

A COMPARATIVE STUDY OF EXPERIMENTAL AND METEORITIC METAL-SULFIDE ASSEMBLAGES

Dante S. LAURETTA[1,2], Daniel T. KREMSER[2] and Bruce FEGLEY, Jr.[1,2]

[1]*Planetary Chemistry Laboratory,*
[2]*Department of Earth and Planetary Sciences,*
Campus Box 1169, Washington University, One Brookings Drive, St. Louis, MO 63130-4899, U.S.A.

Abstract: Sulfide formation via a gas-solid reaction between iron-nickel metal and H_2/H_2S gas mixtures was studied experimentally. This reaction produces distinctive chemical fractionations in both metal and sulfide that can help identify pristine nebular sulfide condensates in meteorites. The resulting sulfide morphology consists of a troilite scale divided into two distinct layers: an inner layer containing small, randomly oriented crystals and an outer layer consisting of large, columnar crystals. A thin band of metal surrounding the unreacted metal core and small metal blebs located in the inner sulfide layer are significantly enriched in nickel relative to the starting metal composition. The stoichiometry of the sulfide is nearly ideal {(Fe+Ni+Co)/S=1} at the metal-sulfide interface but the sulfur content increases with distance from the metal. A significant amount of nickel is present in the sulfide layer and increases in concentration across the sulfide layer. The nickel concentration gradient results from diffusion of nickel ions in the sulfide being faster than that of iron ions. Microprobe analyses on metal-sulfide assemblages in the LL3 unequilibrated ordinary chondrite Allan Hills-764 (ALH-764) do not show these chemical fractionations. Instead, textural and chemical evidence suggests that these meteoritic sulfides were altered during a post accretion heating event.

1. Introduction

One important question in cosmochemistry is how sulfur, the tenth most abundant element, was incorporated from the nebular gas into meteorite parent bodies and planets. If pristine nebular sulfide condensates can be identified in primitive meteorites (chondrites), then the conditions that led to their formation can be better understood. To date only one study, based solely on textural arguments, has claimed to have found pristine nebular sulfides in chondritic material (IMAE, 1994). However, chemical fractionations associated with the sulfurization of an iron-nickel alloy may provide a much better method for the identification of such material.

We present the results of a preliminary experimental study of sulfide formation from the reaction of iron-nickel alloys in H_2/H_2S gas mixtures. This study represents the first attempt to quantify the elemental fractionation that occurs during sulfide formation under solar nebula conditions. We find that the resulting fractionation patterns are distinctive of the sulfurization process and provide important constraints for the identification of pristine nebular sulfide condensates. Furthermore, the composition of sulfide layers formed by a gas-solid reaction with iron-nickel alloys is very sensitive to environmental conditions and has the potential to record pressure, temperature, and sulfur fugacity

conditions at the time of sulfide formation. We compare our experimental products with metal-sulfide assemblages in the LL3 chondrite ALH-764 and find no chemical evidence that they formed by a reaction between iron-nickel metal and a solar composition gas.

2. Experimental and Analytical Procedures

Our experiments are designed to simulate conditions similar to those predicted for regions of the solar nebula where troilite is stable. The metal alloys used in this study were pieces of the Sikhote Alin iron meteorite which were generously provided to us by the Field Museum in Chicago. This meteorite was chosen because it has a composition similar to that of a solar composition iron-nickel alloy (~5% nickel). We found that the nickel content varied from 4.5 to 7.3% nickel with an average composition of 5.5% nickel (all percentages refer to atomic %). The gas mixtures used were Matheson certified standards (accurate to ±2% of the analyzed value) containing 1% H_2S by volume. The H_2S content of this gas is significantly higher than that expected for a solar composition gas (~33 ppmv). However, as shown in Fig. 1, the experimental conditions are still in a region where FeS is the only predicted stable sulfide. The results presented here simulate a nebular environment where the dust-to-gas ratio has been increased by a factor of 30 over solar abundances. Additional studies in gas mixtures closer to solar composition are currently being done to better simulate the nebular environment.

At the beginning of the experiments small pieces of the iron meteorite were suspended by platinum wire harnesses in Deltech resistance wire horizontal tube furnaces. The samples were annealed at 1023 K in prepurified H_2 gas for 24 hours. After annealing the samples were cooled to 923 K. The flow of H_2 was halted and premixed H_2/H_2S gas started to flow across the sample. The reaction was stopped by halting the H_2/H_2S gas flow and flooding the furnace with prepurified N_2. The samples were pulled to the end of the muffle tube assembly and cooled to room temperature within 5 min. Multiple experi-

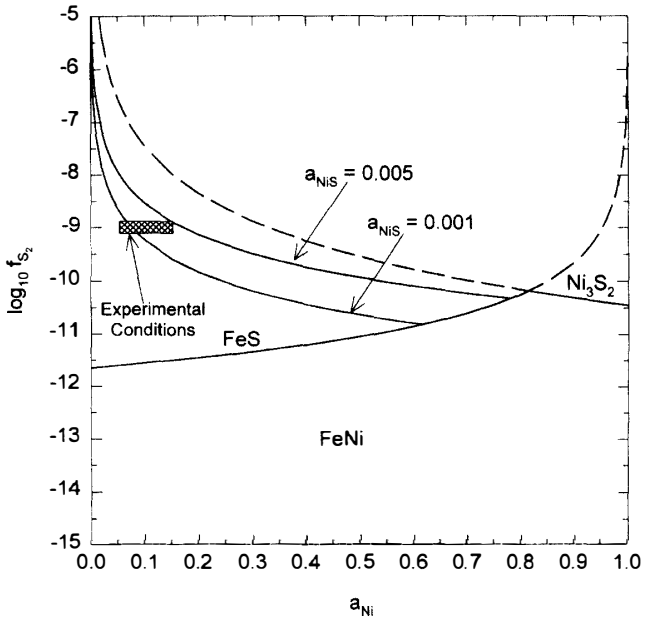

Fig. 1. A graph showing the metal and gas composition conditions of our experiments in relation to the Fe-FeS and Ni-Ni_3S_2 buffers. The dashed lines indicate the metastable extensions of the two buffers. Notice that the sulfur fugacity of the Ni_3S_2 buffer increases with decreasing Ni content and that heazlewoodite (Ni_3S_2) is not stable under our experimental conditions. Also plotted are the curves where 0.1 and 0.5% NiS would dissolve in the FeS layer. The cross-hatched area spans the initial and final nickel content of the metal in our experiments.

ments were done for different time periods to determine the variations in layer morphology and composition as a function of time.

When the experiment was finished the samples were analyzed to obtain structural and compositional information about the sulfide layers. First, the layers were partially removed and powdered for X-ray diffraction analysis. Then, the remainder of the sample was mounted in epoxy and cross-sectioned for analysis by optical microscopy and electron microprobe. X-ray diffraction patterns were obtained using a Rigaku vertical powder diffractometer with Cu-Kα (λ=1.540598 Å) radiation and Materials Data Incorporated software. Electron microprobe analyses were done with the Washington University JEOL-733 electron microprobe equipped with Advanced Microbeam automation. For these analyses, an accelerating voltage of 15 kV was used with 30 nA beam current and a focused beam. X-ray matrix corrections were based on a modified ARMSTRONG (1988) CITZAF routine incorporated into the software. Pyrite was used as the sulfur standard and pure Fe, Ni, and Co metal standards were used for each element respectively.

3. Experimental Results

Our experiments provide information on the variation in the microstructure of a growing sulfide layer with time and the chemical fractionation patterns that result from sulfide formation. Figure 2 is a back scattered-electron image of the sulfide structure from a typical experimental sample and Fig. 3 is a close-up of the metal sulfide interface. The microstructure of the sulfide is similar to that seen in sulfide layers formed during sulfurization of pure iron metal (LAURETTA *et al.*, 1996a, b). The sulfide scale is divided into two distinct layers by a horizontal fracture. The inner layer, at the left of the photo in Figs. 2 and 3, contains small sulfide crystals, blebs of metal, and a large amount of void space. The metal blebs are ubiquitous in the inner layer but are not present in the outer one. The surface of the metal, which was initially polished and flat, is rough and distorted from the reaction. The outer layer of the sample contains large compact crystals and long, vertical cracks extending from the outer edge of the layer to the top of the inner layer.

X-ray diffraction patterns of the sulfide layers show that only troilite is present. However, as shown in Fig. 4, electron microprobe analyses of the sulfide layers reveal large variations in the stoichiometry and nickel content of the sulfide. The variation in stoichiometry across the sulfide layer is expressed as the ratio of iron, nickel, and cobalt to sulfur (Fe+Ni+Co/S). This ratio describes the deviation from ideal stoichiometry ($1-\delta$) as given in the formula $(Fe,Ni,Co)_{1-\delta}S$. At the metal interface the composition of the sulfide is nearly stoichiometric (δ–0) due to equilibrium with the metal phase. However, the sulfur content increases with distance from the metal and δ reaches a maximum value of 0.05 at the outer edge of the sulfide layer. This type of variation has been reported previously by investigators studying sulfurization of pure iron and is indicative of sulfide formation via a gas-solid reaction (LAURETTA *et al.*, 1996a; NARITA and NISHIDA, 1973; ORCHARD and YOUNG, 1989; WAGNER, 1951). The nickel content in the sulfide is expressed as the ratio of nickel to total metal in the sulfide (Ni/Fe+Ni+Co). The nickel mole fraction in the sulfide also increases with distance from the metal, ranging from 0.02 at the metal-sulfide interface to 0.06 at the outer edge of the layer, a value larger

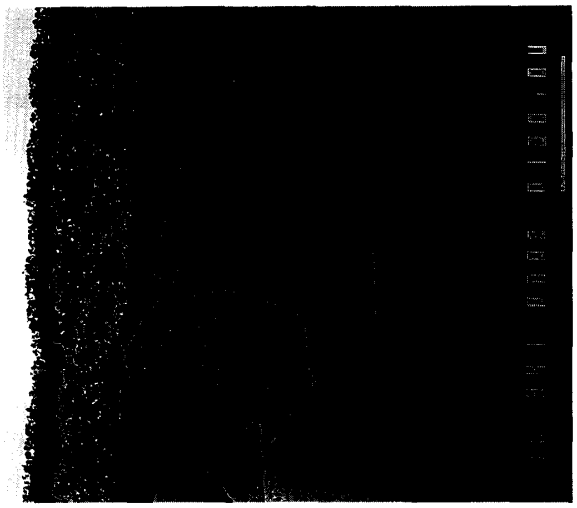

Fig. 2. Back scattered-electron image taken at 240× magnification illustrating a typical run product of iron-nickel alloy sulfurization. The remaining metal is seen along the far left edge. This layer formed on a piece of Sikhote Alin heated at 923 K for 24 hours in an H_2-H_2S gas mixture containing 1% H_2S. Two distinctive sulfide layers are visible. The scale bar=100 microns.

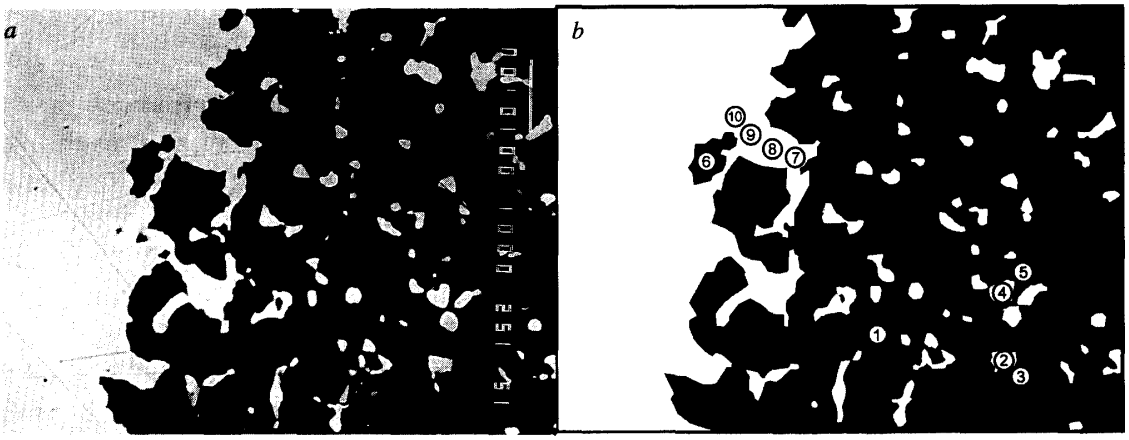

Fig. 3. a) Back scattered-electron image taken at 1500× magnification of the metal-sulfide interface of one of our experimental samples. The original metal is seen along the far left edge. The sulfide formed on a piece of the Sikhote Alin meteorite at 923 K for 96 hours in an H_2-H_2S gas mixture containing 1% H_2S. The scale bar=10 microns. b) Drawing of the interface showing location of electron microprobe analyses. The numbered dots correspond to the compositions given in Table 1.

Table 1. Selected microprobe spot analyses from sample SA9.

Point	X-Fe	X-Ni	X-Co	X-S
1	0.488	0.009	BDL	0.501
2	0.609	0.367	0.014	0.010
3	0.490	0.010	BDL	0.498
4	0.636	0.312	0.012	0.040
5	0.490	0.010	BDL	0.498
6	0.494	0.009	BDL	0.496
7	0.794	0.185	0.009	0.013
8	0.847	0.146	0.006	BDL
9	0.934	0.060	0.005	BDL
10	0.943	0.050	0.006	BDL

BDL-Below detection level.

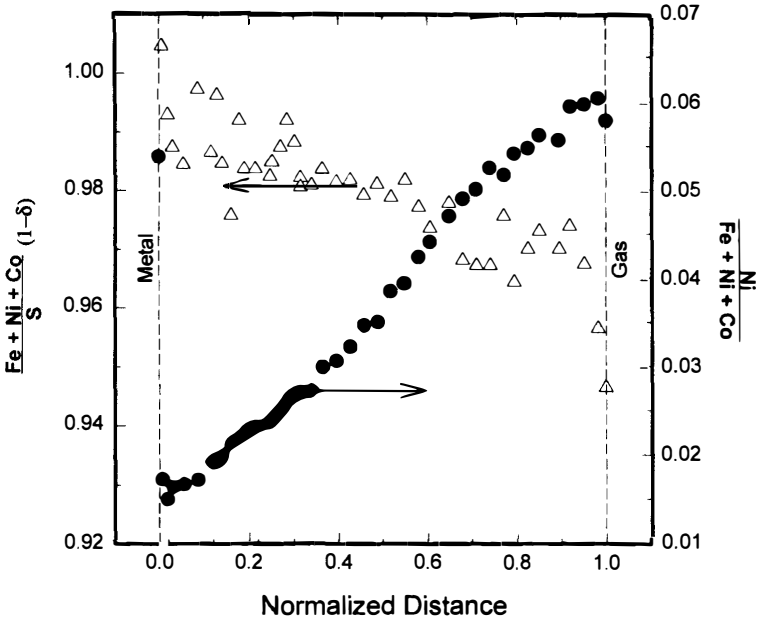

Fig. 4. Typical elemental compositions in an experimentally produced sulfide layer. Open triangles illustrate the variation in sulfide stoichiometry and correspond to the y-axis on the left while the solid circles represent the variation in nickel content across the layer and correspond to the y-axis on the right.

than that in the starting metal alloy. We also performed detailed analyses of the metal and sulfide near the interface. The locations of these analyses are indicated in Fig. 3b and the results at each point are presented in Table 1. There is a sharp gradient in the nickel content of the metal with values ranging from the initial composition of 5% to 18.5 % nickel over a distance of 10 microns. In addition, the small metal blebs in the inner sulfide layer contain as much as 37% nickel.

4. Reaction Mechanisms

The information obtained from our experiments leads us to propose the following model for the mechanisms involved in sulfide formation via a gas-solid reaction. Previous studies of iron metal sulfurization show that the crystals in the outer layer are the first to form (Lauretta *et al.*, 1996a). During the early stages the chemical reaction takes place at the sulfide-gas interface and the reaction rate is limited by diffusion of Fe^{2+} ions through the outer sulfide layer (Condit *et al.*, 1974). The removal of Fe atoms from the metal creates a gap between the two phases. The sulfide must deform towards the metal to maintain contact. When the plastic deformation limit of the sulfide is reached vertical cracks form. The gas then has direct access to the metal surface and an inner sulfide layer starts forming.

Under the experimental conditions studied here, the composition of the first sulfide to form is nickel-free FeS. Equilibrium with the metal fixes the composition of the iron sulfide at the metal-sulfide interface at a metal-to-sulfur ratio of unity (δ=0). Once a sulfide layer has formed and the metal is no longer in contact with the gas the nickel content of the sulfide at the metal interface is controlled by equilibrium with the metal. This is expressed by the reaction:

$$Fe+NiS=FeS+Ni, \quad (1)$$

and the nickel content of the sulfide can then be expressed as:

$$a_{NiS}=\frac{a_{FeS}a_{Ni}}{a_{Fe}}\cdot\frac{1}{K_1}, \quad (2)$$

where a_i is the activity of species i and K_1 is the equilibrium constant for eq. (1) which is inversely proportional to temperature. It is therefore possible to determine an equilibrium temperature by measuring the nickel content of the metal and sulfide at this interface. The outer edge of the sulfide, however, is in equilibrium with the external H_2-H_2S atmosphere which in these experiments has a higher sulfur fugacity than that fixed by the metal-sulfide boundary. Thus, the outer edge of the sulfide is more sulfur-rich and therefore has a lower metal-to-sulfur ratio.

The nickel content of the metal does not remain constant throughout the course of the reaction. The continuous loss of iron from the metal causes the metal that is left behind to become enriched in nickel. This enrichment does not extend into the bulk metal phase but is limited to a very narrow band around the metal core. It can be seen from eq. (2) that the nickel content of the sulfide at the metal-sulfide interface is controlled only by the composition of the metal at the metal-sulfide interface and the temperature. Thus, as the reaction proceeds, the increase in the nickel content of the metal drives more nickel into the sulfide phase.

However, the nickel content of the sulfide is not constant. Once in the sulfide nickel is driven towards the sulfide-gas interface by the nickel concentration gradient. WAGNER (1969) showed that the ratio of the concentration of two diffusing cation species in a solid solution scale layer will vary if their relative diffusion coefficients are significantly different. Previous studies of iron and nickel diffusion rates in iron sulfide indicate that Ni^{2+} diffuses almost twice as fast as Fe^{2+} (ORCHARD and YOUNG, 1989). This will cause a higher relative amount of nickel to reach the outer edge of the sulfide layer than is at the metal-sulfide interface. The result of this process will be a variation of the mole fraction of nickel in the sulfide with increasing distance from the metal.

5. Analyses of Meteoritic Sulfides

Our experiments show that sulfide formation via a gas-solid reaction with iron-nickel alloys leaves extensive textural and chemical evidence of the process. IMAE (1994) recently claimed to have identified pristine nebular sulfide condensates in the LL3 chondrite ALH-764 using only textural arguments. We examined a thin section of this meteorite (ALH-764,71-4), which was kindly provided by the National Institute of Polar Research in Tokyo, by optical microscopy and electron microprobe analysis to look for chemical evidence of the sulfurization process. We examined all 66 metal-sulfide assemblages in this thin section. The majority (33) of them occur as fine grained rims surrounding larger, broken up silicate chondrules that appear to have been shocked after their formation. An example of this morphology is shown in Fig. 5. There are 12 occurrences of anhedral sulfide and metal blebs in the matrix and 7 other sulfide assemblages

are present within other chondrules. An example of metal and sulfide blebs contained within a larger silicate chondrule is shown in Figs. 6a and 6b. Eight of the metal-sulfide grains occur as intergrowths of metal, sulfide, and silicate. We found only six metal-sulfide assemblages having a sulfide rim surrounding a metal grain. Intuitively this is the morphology one would expect as a result of sulfide formation via a gas-solid reaction.

IMAE (1994) used the criterion of a fracture dividing a sulfide rim around a metal grain into two distinct layers as his sole means of identifying nebular sulfide condensates. This is a common feature expected from gas-solid sulfurization products and has been observed in the study of sulfurization of pure iron metal (LAURETTA and FEGLEY,

Fig. 5. Reflected light photomicrograph (12.5× magnification) of a silicate chondrule (from ALH-764) rimmed by metal and sulfide. The field of view is 2 mm.

a)

b)

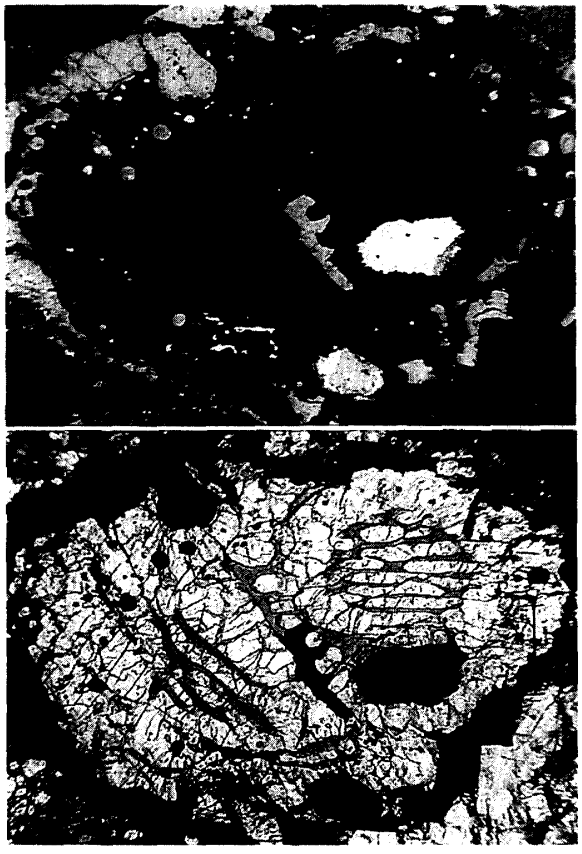

Fig. 6. a) Reflected light and b) transmitted light photomicrographs (25× magnification) of a silicate chondrule (from ALH-764) containing both metal and sulfide assemblages. The field of view is 1 mm.

1994a,b; FRYT *et al.*, 1979; WORRELL and TURKDOGAN, 1968). Imae's claim that a two layer sulfide rim is a common feature of grains in ALH-764 is not supported by our survey as we were only able to locate one grain with such a morphology, shown in Fig. 7. This assemblage has a central core of iron-nickel metal, the majority of which is kamacite. Two small grains of taenite, both with average composition of ~47% nickel, are also contained within the metal. The metal is surrounded in part by a two layer rim of essentially nickel free troilite. The dark grain at the left edge of the metal has been identified as an iron oxide containing a small amount of sulfur. It is interesting to note that the sulfide rim extends beyond the metal core and surrounds the oxide.

Since this grain has the morphology that IMAE (1994) claims to indicate formation via gas-solid reaction, we performed extensive optical microscopy and electron microprobe analyses of this assemblage. The points analyzed by the electron microprobe are shown in Fig. 8. The average thickness of the sulfide layer is 40 microns and the average radius of the metal core is 80 microns. We compared the cross-sectional area fraction of

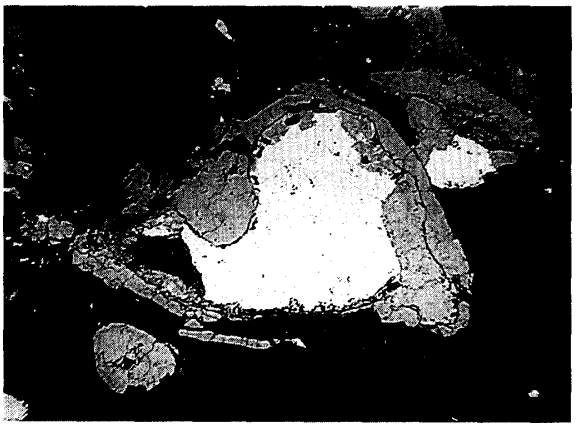

Fig. 7. Reflected light photomicrograph (50× magnification) of a sulfide rimmed metal grain from ALH-764. The triangular shaped, small dark grain at the left edge of the metal is an iron oxide. The two layer structure of the sulfide rim is clearly developed. The field of view is 0.5 mm.

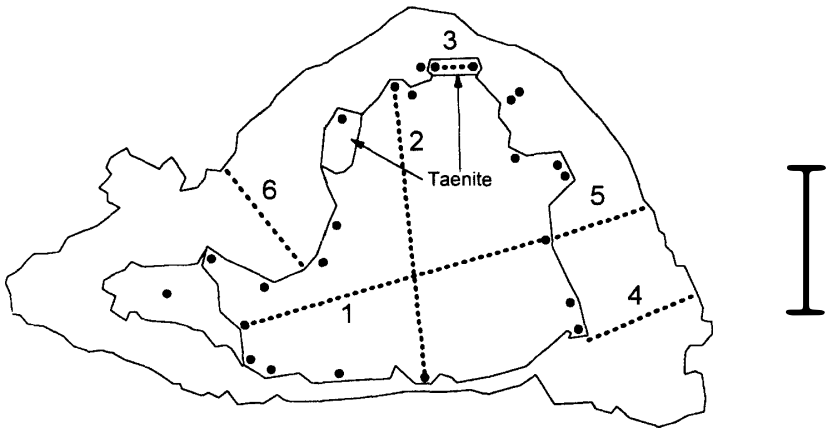

Fig. 8. Sketch of the metal-sulfide assemblage shown in Fig. 7. Solid circles indicate locations of electron microprobe analyses. The numbered dashed lines indicate traverses done across metal and sulfide. The scale bar=80 microns.

the sulfide and metal phases and, assuming that the volume fraction of each is equal to its cross-sectional area fraction (KINGERY *et al.*, 1976), determined that 53% of the metal initially present has reacted to form the sulfide. Condensation calculations indicate that an Fe-Ni alloy condensed from a solar gas will have solar composition ($Fe_{0.95}Ni_{0.05}$) by the time troilite becomes stable (KELLY and LARIMER 1976; SEARS 1978). The troilite surrounding this grain is essentially nickel free and therefore all of the nickel must still be in the metal. Mass balance implies that the remaining bulk metal should have an average composition of 11% nickel. However, we find an average composition of only 6.5% nickel. Furthermore, if the sulfide formed by gas-solid reaction then the metal near the interface should be enriched in nickel as indicated by our experimental results. We performed microprobe analyses near the reaction interface (~5 microns from the sulfide) all around the metal grain. At every one of these locations the nickel content of the metal is significantly less than that of the bulk metal grain with the exception of the two small taenite grains contained within the metal. Calculations of the total nickel content of the metal suggest that there is not enough nickel contained within these two grains to account for the deficit in nickel content of the metal. There is no evidence of a thin band of nickel enriched metal at the outer edge of the metal or small, nickel-rich blebs of metal in the sulfide as would be expected in the product of a gas-solid reaction.

We performed two traverses across the kamacite grain (traverses 1 and 2) and one across a taenite grain (traverse 3). The results of the traverses are shown in Fig. 9. The nickel content of the kamacite increases toward the center of the grain, a pattern which is common among kamacite grains in chondrites (NAGAHARA 1979; WOOD 1967). The total nickel content of this grain ranges from 5.5% at the outer edge of the grain to a maximum value of 6.2% at the center. The nickel content of the taenite grain is divided into two distinct regions, one containing 50% nickel and the other 40% nickel.

In addition to analyzing the metal core of the grain we also performed extensive analyses of the sulfide rim. We analyzed the troilite in contact with the grains of taenite as well as sulfide near the kamacite interface to determine the equilibrium temperature

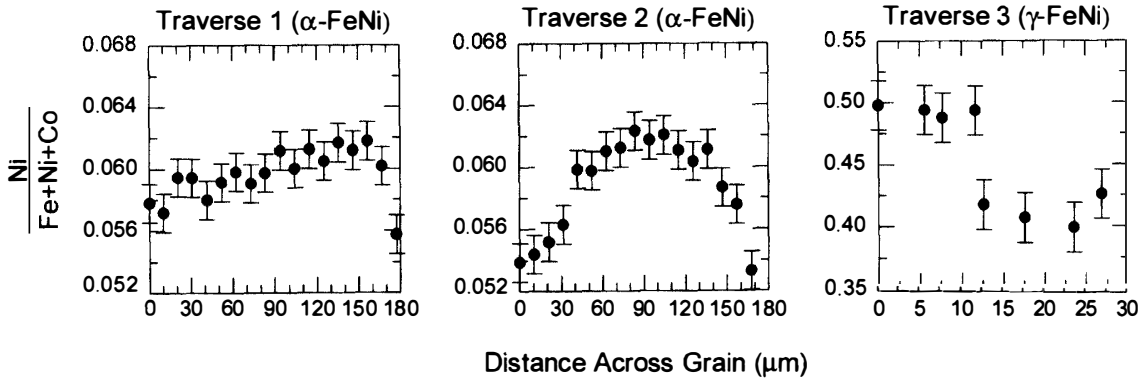

Fig. 9. Elemental composition of the metal grain shown in Fig. 7. Analyses of the kamacite show increasing nickel content towards center of the grain while the taenite has two distinct nickel concentrations. No evidence of nickel enrichment at the outer edge of the metal was found as would be expected from FeNi alloy sulfurization by H_2-H_2S gas. The total distance covered in traverse 1 is 172 microns; in traverse 2 is 157 microns; and in traverse 3 is 27 microns. The 1σ uncertainty is ±2%.

of the assemblage. BEZMEN *et al.* (1978) presented formulas for calculating the equilibrium temperature from metal-sulfide assemblages. We revised their formulas using updated thermodynamic data and calculated a temperature of 818 K for the kamacite-troilite assemblage and a temperature of 983 K for the taenite-troilite contact. These temperature are well above the troilite condensation temperature in the solar nebula of 713 K (LAURETTA *et al.*, 1996a). These results imply that if the sulfide layer formed by a gas-

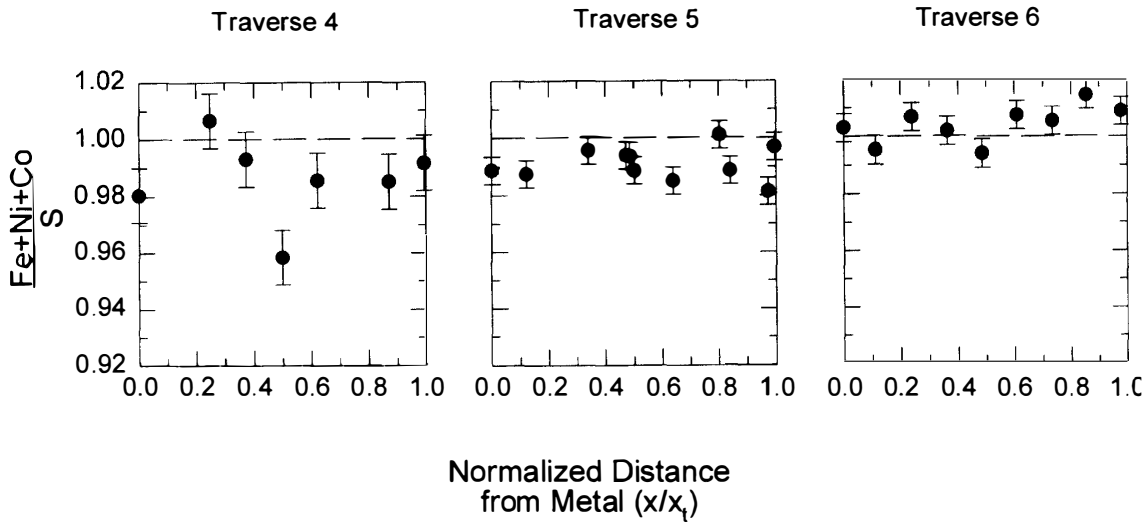

Fig. 10. Variation in stoichiometry across the sulfide rim along the three traverses shown in Fig. 8. The sulfide composition at the metal-sulfide interface is not always ideal and there is no variation in the sulfur content with increasing distance from the metal. The total distance covered in traverse 4 is 62 microns; in traverse 5 is 53 microns; and in traverse 6 is 71 microns. The 1σ uncertainty is ±1.5%.

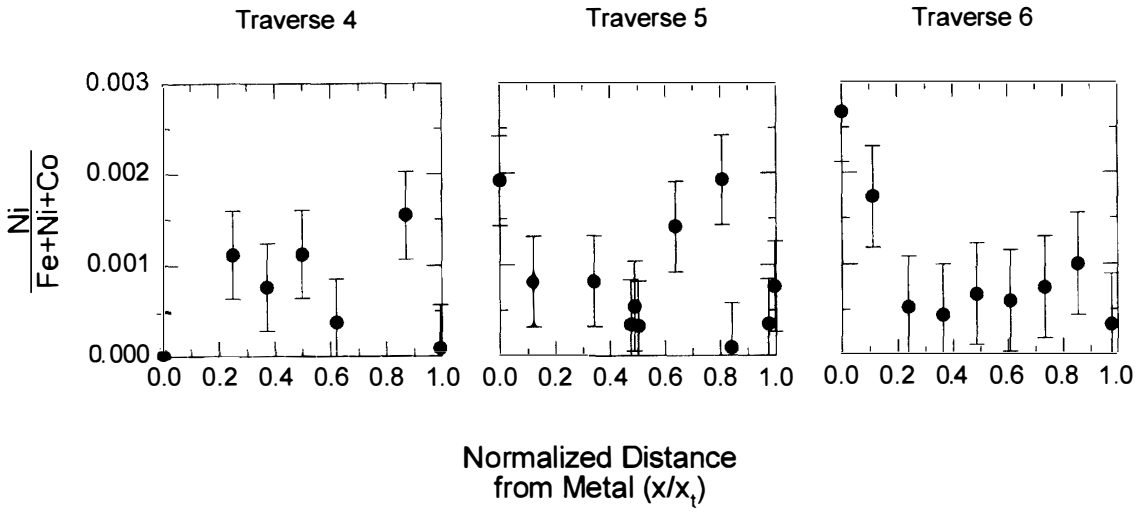

Fig. 11. Variation in nickel content across the sulfide rim along the three traverses shown in Fig. 8. Very little nickel is present in the sulfide and no compositional gradient with distance from the metal-sulfide interface is apparent. There is no evidence to suggest sulfide formation via a gas-solid reaction. The 1σ uncertainty is ±57%.

solid reaction then it must have formed in a region where the dust-to-gas ratio was enriched relative to solar composition allowing troilite to condense at a higher temperature. Since our experiments simulate an enriched solar nebula gas our results are directly applicable to this assemblage.

To determine if there is any variation in the sulfide content away from the metal, the sulfide layers were analyzed by performing three microprobe traverses from the metal to the outer edge of the sulfide. The results of the three traverses (traverse 4–6) are presented in Fig. 10. We found that the sulfide composition at the metal-sulfide interface is not always that expected from equilibrium with the metal (δ=0). Also, the layers do not show any sulfur enrichment at the outer edge of the crystals. In fact, traverse 6 appears to be slightly enriched in metal at the outer edge of the sulfide relative to the composition at the metal-sulfide interface. These profiles are not similar to those observed in the products of iron-nickel alloy sulfurization. Figure11 plots the mole fraction of nickel in the sulfide layer versus distance from the metal interface for the same set of traverses. The amount of nickel in the sulfide is extremely low, ranging from zero to three tenths of a percent nickel. The values scatter randomly and there does not appear to be any trend with distance. In contrast, the experimental samples contain more than one percent nickel in the sulfide at the metal interface and the nickel content increases with distance from the interface. This implies that the chemical signature of the sulfurization process has been erased in the meteoritic metal-sulfide assemblage.

6. Formation Scenarios for ALH-764 Sulfides

Since the metal-sulfide assemblage that we analyzed does not show any chemical evidence for formation by gas-solid reaction we suggest that the sulfide rims surrounding the metal grains in ALH-764 may have been altered during a post-accretion heating event. The metal-sulfide rims surrounding the silicate grains (Fig. 5) are similar to those described by GROSSMAN and WASSON (1987) for the Semarkona chondrite (LL3). They suggest that the metal-sulfide rims formed when droplets of a metal-sulfide melt migrated to the chondrule surface. A later reheating event allowed the material to be incorporated into the matrix-like material that had accreted onto the surface. The sulfide blebs contained within chondrules (Fig. 6) may represent melt that did not migrate to the exterior of the chondrule. Furthermore, experiments done by WOOD (1967) have shown that both sulfur and nickel are extremely mobile through solid phases in heated chondritic material. In his experiments nickel preferentially concentrated in the metal phases while sulfur attacked the metal and formed nickel-free sulfide rims around the metal grains. The high equilibrium temperatures calculated from the composition of the metal-sulfide assemblage also support this theory of formation. Thus, the same heating event that formed the rims around the silicate chondrules could also have led to the formation of the sulfide rims around the metal grains.

7. Formation of Two-Layer Sulfide Rims on Meteorite Parent Bodies

The strongest evidence presented by IMAE (1994) for formation of the sulfide rimmed metal grains in ALH-764 by gas-solid reaction in the solar nebula is the presence of a

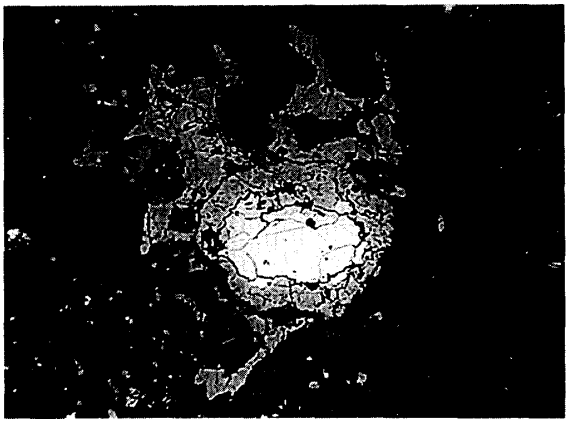

Fig. 12. Reflected light photomicrograph (25× magnification) of a sulfide rimmed metal grain in the CO3 chondrite Y-791717. A chance contact between this grain and other sulfide-rimmed silicate grains create the appearance of a two-layer sulfide rim. A similar morphology is seen in Fig. 1b of IMAE (1994). The field of view is 1 mm.

fracture dividing the sulfide into two distinct layers. However, we feel that the two layer sulfide structure could result from a variety of processes. If the chondrite experienced several episodes of reheating to temperatures high enough to mobilize sulfur through the solid matrix then several distinct sulfide rims could form around the metal grains in the matrix of the chondrite. In addition, the two layer structure could form during a single heating event if the sulfide layer was disrupted or pulled away from the metal grain during its formation. Many of the silicate chondrules in this meteorite appear to have undergone a shock event sometime in their past. It is possible that such an event would break up a sulfide rim giving the appearance of a two layer structure. Another phenomena that we have observed in the CO3 chondrite Yamato-791717 (Y-791717) is contact between two sulfide rims surrounding separate silicate and metal grains. Several such assemblages in close contact can give the appearance of a two layer rim around the grain near the center of the assemblage (Fig. 12). We propose that such an assemblage created the two layer sulfide rim in the grain shown in Fig. 1b of IMAE (1994). All these scenarios plausibly explain the formation of a two-layer sulfide rim surrounding a metal grain. However, evidence from the sulfide rims around the silicate chondrules and the high equilibrium temperature of the metal-sulfide assemblage suggests that the sulfide rims are the result of a post accretion heating event on the LL3 meteorite parent body.

8. Summary

Our experimental studies of iron-nickel alloy sulfurization show that several important elemental fractionations occur that can be used to determine whether sulfide assemblages observed in chondrites formed via a gas-solid reaction in the solar nebula. These fractionations include the presence of a thin band of nickel-enriched metal along the metal-sulfide interface and small, nickel-rich metal blebs located in the inner layer of the sulfide. The stoichiometry of the sulfide at the metal interface is nearly ideal but the sulfur content increases away from the metal. A significant amount of nickel is present in the sulfide due to equilibrium at the metal-sulfide interface. The amount of nickel in the sulfide is controlled by the composition of the metal at the metal-sulfide interface and the formation temperature but is independent of the sulfur fugacity in the gas. The relatively faster diffusion of nickel than iron in the sulfide layer results in a large nickel

concentration gradient with nickel content increasing away from the metal-sulfide interface.

The sulfide rimmed metal grains in the unequilibrated ordinary chondrite ALH-764 do not display any of the elemental fractionations seen in our experimental samples even though one of these grains has a two layer structure, which is a common feature in gas-solid sulfurization products. However, textural grounds alone are insufficient to determine whether a metal-sulfide assemblage in chondrites is a pristine condensate. Clear identification requires the presence of the elemental fractionations associated with sulfurization. We propose that other processes must have produced the two layer sulfide rim which was only observed in one assemblage in the thin section we studied. Other assemblages in this meteorite, particularly the metal-sulfide rims surrounding larger silicate chondrules suggest that this meteorite experienced a post accretion heating event. This event could also be responsible for the formation of the sulfide rims around the metal grains due to sub-solidus sulfur mobilization through matrix material.

Acknowledgments

This work was supported by NASA Grant NAGW-3070. We acknowledge advice from K. LODDERS. We thank the Field Museum in Chicago for providing the samples of Sikhote Alin used in the sulfurization experiments and the National Institute for Polar Research in Tokyo for loaning us the thin section of ALH-764. Dr. TSUCHIYAMA and an anonymous referee provided constructive reviews.

References

ARMSTRONG, J.T. (1988): Quantitative analysis of silicate and oxide minerals: Comparison of Monte-Carlo, ZAF and Phi-Rho-Z procedures. Microbeam Analysis, 239–246.

BEZMEN, N.I., LOTOV, V.S. and OSADCHIY, Ye.G. (1978): Distribution of nickel between troilite and metallic iron as a mineralogical thermometer. Geochem. Int., **15**, 120–127.

CONDIT, R.H., HOBBINS, R.R. and BIRCHENALL, C.E. (1974): Self-diffusion of iron and sulfur in ferrous sulfide. Oxid. Met., **8**, 409–455.

FRYT, E.M., BHIDE, V.S., SMELTZER, W.W. and KIRKALDY, J.S. (1979): Growth of the iron sulfide ($Fe_{1-\delta}S$) scale on iron at temperatures 600°–1000°C. J. Electrochem. Soc., **126**, 683–688.

GROSSMAN, J.N. and WASSON, J.T. (1987): Compositional evidence regarding the origins of rims on Semarkona chondrules. Geochim. Cosmochim. Acta, **51**, 3003–3011.

IMAE, N. (1994): Direct evidence of sulfidation of metallic grain in chondrites. Proc. Jpn. Acad., **70**, Ser. B, 133–137.

KELLY, W.R. and LARIMER, J.W. (1976): Chemical fractionations in meteorites- VIII. Iron meteorites and the cosmochemical history of the metal phase. Geochim. Cosmochim. Acta, **41**, 93–111.

KINGERY, W.D., BOWEN, H.K. and UHLMAN, D.R. (1976): Introduction to Ceramics. New York, J. Wiley, 1032p.

LAURETTA, D. and FEGLEY, B., Jr. (1994a): An experimental study of iron sulfide formation kinetics in H_2-H_2S gas mixtures and application to iron sulfide condensation in the solar nebula. Lunar and Planetary Science XXV. Houston, Lunar Planet Inst., 773–774.

LAURETTA, D.S. and FEGLEY, B., Jr. (1994b): Kinetics and grain growth mechanism for troilite formation on iron metal in H_2-H_2S gas mixtures. Papers Presented to the 19th Symposium on Antarctic Meteorites, May 30–June 1, 1994. Tokyo, Natl Inst. Polar Res., 62–65.

LAURETTA, D.S., KREMSER, D.T. and FEGLEY, B., Jr. (1996a): The rate of iron sulfide formation in the solar nebula. Icarus (in press).

LAURETTA, D.S., FEGLEY, B., Jr., LODDERS, K. and KREMSER, D.T. (1996b): The kinetics and mechanism of iron sulfide formation in the solar nebula. Proc. NIPR Symp. Antarct. Meteorites, **9**, 111–126.

NAGAHARA, H. (1979): Petrological study of Ni-Fe metal in some ordinary chondrites. Mem. Natl Inst. Polar Res., Spec. Issue, **15**, 111–122.

NARITA, T. and NISHIDA, K. (1973): On the sulfur distribution in FeS scale formed on pure iron at 700°C. Trans. Jpn. Inst. Met., **14**, 447–456.

ORCHARD, J.P. and YOUNG, D.J. (1989): Sulfidation behavior of an iron-nickel alloy. J. Electrochem. Soc., **136**, 545–550.

SEARS, D.W. (1978): Condensation and the composition of iron meteorites. Earth Planet. Sci. Lett., **41**, 128–138.

WAGNER, C. (1951): Atom Movements. Ohio, American Society for Metals, 153–173.

WAGNER, C. (1969): The distribution of cations in metal oxide and metal sulphide solid solutions formed during the oxidation of alloys. Corros. Sci., **9**, 91–109.

WOOD, J.A. (1967) Chondrites: Their metallic minerals, thermal histories, and parent planets. Icarus **6**, 1–49.

WORRELL, W.L. and TURKDOGAN, E.T. (1968): Iron sulfur system part II. Rate of reaction of hydrogen sulfide with ferrous sulfide. Trans. AIME, **242**, 1673–1678.

(Received July 31, 1995; Revised manuscript accepted November 2, 1995)